Evaluating Method of Deformation at Losing Point of Axial Load Carrying Capacity of RC Columns

Daisuke Kato[1], Yudai Miyajima[2] and Yukiko Nakamura[3]

[1] Professor, Dept. of Architecture, Faculty of Engineering, Niigata University, Niigata, Japan
[2] Graduate Student, Dept. of Architecture, Faculty of Engineering, Niigata University, Niigata, Japan
[3] Lecturer, Dept. of Architecture, Faculty of Engineering, Niigata University, Niigata, Japan

Abstract

RC buildings often suffer severe damage, including pancake-type total collapse, during strong earthquakes. The objective of this study is to find a way to prevent pancake-type collapse in old RC buildings during strong earthquakes. In 2006, the authors conducted static loading tests on RC column specimens failing in shear and proposed an equation for evaluating the lateral deflection angle at the losing point of axial load carrying capacity. In this study, first, the equation was reexamined using data for specimens with a wider range of parameters. Comparison with this new experimental data showed that the equation is effective for conservative evaluation. Second, the applicability of the equation to RC columns failing in flexure was also examined. For this, the lateral deflection angle of columns failing in flexure was obtained by adding the flexural component to the shear component proposed already. The proposed method was found to be effective. Finally, a trial evaluation of the axial deformation at the losing point of the axial load carrying capacity was performed, and the equation was found to be effective, though with some exceptions.

Keywords: reinforced concrete structure, column, axial load carrying capacity, reinforcing detail, shear failure

1. Introduction

Many RC buildings have suffered considerable damage, including pancake-type total collapse, during strong earthquakes. The objective of this study is to find a way to prevent pancake-type collapse in old RC buildings during strong earthquakes. For this purpose, some studies have been performed on the axial load carrying capacities of RC columns (Pujol et al. (2000), Moehle et al. (1999), Nakamura et al. (2002)). The authors also conducted static loading tests on RC columns failing in shear and proposed an equation for evaluating the lateral deflection angle at the losing point of the axial load carrying capacity (Kato et al. (2006)). The "losing point of the axial load carrying capacity" is defined as "the point where a column specimen cannot sustain the scheduled constant axial load during the loading test," and it is sometimes abbreviated as the axial capacity point in this report.

The equation proposed in 2006 is reexamined herein using data for specimens with a wider range of parameters. Further, the applicability of the equation to RC columns failing in flexure was examined. Trials to evaluate the axial deformation at axial capacity point were also carried out.

Contact Author: Daisuke Kato
Professor, Dept. of Architecture, Faculty of Engineering, Niigata University
Ikarashi 2-no-cho 8050, Nishi-ku, Niigata 950-2181, Japan
Tel: +81-025-262-7205 Fax: +81-025-262-7205
e-mail: dkato@eng.niigata-u.ac.jp

(The publisher will insert here: received, accepted)

2. Summary of evaluation equation proposed by Kato et al. (2006)

In this section, the authors provide a summary of the equation for evaluating the lateral deflection angle at the axial capacity point for RC columns failing in shear, which was proposed by Kato et al. in 2006, and shown here.

The equation is as follows:

$$R_{axis,s} = \frac{0.027}{\eta} \qquad (\eta = \frac{{}_eN}{P_{fr,cal}}) \tag{1}$$

$${}_eN = N + Q\frac{\sin^2\theta - \cos^2\theta - 2\mu\cdot\sin\theta\cdot\cos\theta}{\sin\theta\cdot\cos\theta - \mu\cdot\cos^2\theta} \tag{2}$$

$$P_{fr,cal} = P_{fro}\cdot(1 - 0.5\cdot\frac{S}{D})\cdot R_d \tag{3}$$

$$P_{fro} = b\cdot D\cdot p_w\cdot\sigma_{wy}\frac{\sin\theta\cdot\cos\theta + \mu\cdot\sin^2\theta}{\sin\theta\cdot\cos\theta - \mu\cos^2\theta} + A_s\cdot\sigma_y \tag{4}$$

where N is the axial load; Q is the shear force at the

losing point of the axial load capacity and can be replaced by the shear strength Q_s shown later; μ is the coefficient of friction on a slip surface, which is 0.77; θ is the slip angle, which is 60°; b is the width; D is the depth of the cross section; p_w, σ_{wy}, and S are the shear reinforcement ratio, yield strength, and spacing respectively; A_s and σ_y are the gross cross-sectional area and the yield strength of the main reinforcement respectively; and R_d is the effectiveness factor of the reinforcing details. $R_d = 1$ for a welded tie hoop and $R_d = 0.8$ for a 90° hook (extra length = 4d). Equation (1) is derived from the test data within the p_w range of 0.4%–0.68%, and $0.7 < \eta < 2.8$.

The concept of the equation is based on the idea that the deflection at the losing point of the axial load capacity does not depend on the commonly used axial load ratio using the subjected axial load (N) and the axial load strength of the section ($bD\,\sigma_B$) but depends on the equivalent axial load ratio using the equivalent axial load ($_eN$) and the axial load resisted by friction at the starting point of the sliding of the column ($P_{fr,cal}$). The equivalent axial load ($_eN$) is the normal component of the sliding force along the inclined surface caused by a shear crack. Figure 1 shows this condition. In contrast, Figure 2 shows the concept of the axial load resisted by friction at the starting point of the sliding of the column. In this figure, point E represents the starting point of the condition where the axial force is resisted by friction only along the inclined crack surface. Moreover, the figure shows how to determine point E using experimental data. The axial load $P_{fr,cal}$ for calculation was empirically obtained using experimental data.

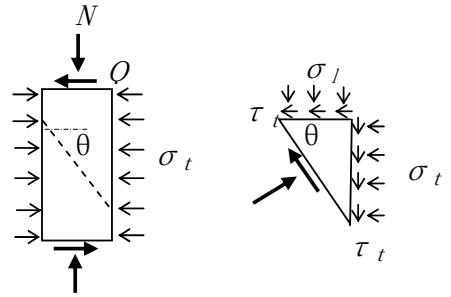

Fig. 1 Basic concept of stress condition of concrete

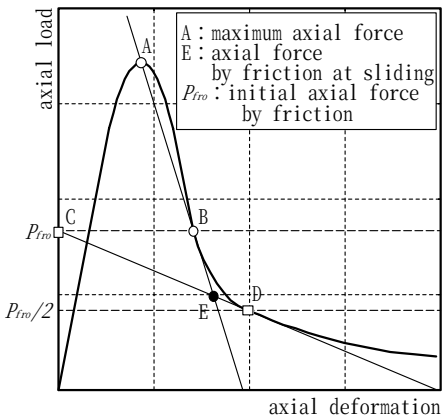

Fig. 2 Modeling of axial load – axial deformation behavior of specimen subjected to uni-axial loading and the concept of axial load resisted by friction at starting point of sliding

3. Specimens examined for axial load carrying capacity

3.1 Tests to derive Equation (1)

Table 1(a) shows the properties of the test series that were used for proposing Eq. (1). Table 2(a) shows the subjected axial load and the test results of each specimen. The objective of these tests was to examine the effects of various reinforcing details on the axial load carrying capacities of RC columns failing in shear. The details of tests were reported by Kato et al. (2006), and the test data for the P and H series were reported by Kato et al. (2004) in English. The test results include the lateral deflection and axial deformation at the axial capacity point, which were defined as maximum values observed during the loading tests. The lateral deflection angle was obtained as the lateral deflection divided by the column height (H). However, it must be noted that the axial strain was obtained as the axial deformation divided by the depth of the column section (D). This is because plastic axial deformation occurs within the range of the column section, not all along the column height.

Table 1 Properties of test specimens of test series
(a)conducted from 2002 to 2006 by the authors

series name of specimen	dimension		main bar		hoop				concrete strength Fc [N/mm^2]
	section [mm^2]	height [mm]	main bar	yield strength σy [N/mm^2]	hoop bar	hoop type*	spacing S[mm]	yield strength σwy [N/mm^2]	
P	180 × 180	360	4-D10	383	2-D6	type A1	70	316	35.2
H					2-D6	type B1			
W				377	2-D6	type C		343	23.4
S					2-D6	type A2		396	
W52				383	2-D6	type C	52	354	28.2
W90							90		
D13W			4-D13	335			70	335	26.7
D13S					2-D6	type A2			
φ4W			4-φ4	502	2-D6	type C			
WH			4-D10	371				316	32.2
SH					2-D6	type A2			
WL					2-D6	type C			19.1
SL					2-D6	type A2			

(b)conducted after 2006 by the authors

series name of specimen	dimension		main bar		hoop				concrete strength Fc [N/mm^2]
	section [mm^2]	height [mm]	main bar	yield strength σy [N/mm^2]	hoop bar	hoop type*	spacing S[mm]	yield strength σwy [N/mm^2]	
H52LL	180 × 180	360	4-D10	312	2-D4	type B2	52	420	16.8
H90LL							90		
S52L					2-D4	type B2	52		15.6
I52L			8-D6	333	3-D4	type B2			
V78LL	270 ×270	540	4-D16	375	2-D6	type B2	78	345	14.1
V135LL							135		
L52LL	180 ×180		4-D10	364	2-D4	type B2	52	432	
L90LL							90		

hoop type* type A1 : 90deg hook with 6d extra length type B1 : 135deg hook with 8d extra length
type A2 : 90deg hook with 4d extra length type B2 : 135deg hook with 6d extra length
type C : welded

3.2 Tests conducted after 2006

After proposing Eq. (1), the authors conducted additional tests for the columns that failed in shear in order to verify the validity of Eq. (1) for a wide range of variables. Table 1(b) shows the properties of the test series, and Table 2(b) shows the subjected axial load and the test results of each specimen. One of the parameters of these tests was the size of the section, which should be examined in order to improve the feasibility of the equation.

Although details of tests were reported by Miyajima et al. (2007 and 2008), the outline of the testing method is given in this section. Figure 3 shows the examples of cross section and reinforcing details. The loading equipment is shown in Figure 4. Although the size of the test specimens was 180 × 180 × 1200 mm in these examples, the test section was a central section of 360 mm because both ends of the test specimens were covered by foundation pieces as shown in Figure 4. The parameters of the test were the section size, subjected axial load ratio, hoop lateral tie diameter (shear reinforcement ratio), and detail of hoop lateral tie (135° hook, 90° hook, presence of tie). All specimens were designed to fail in shear. The axial deformation was measured at two points on both sides of the test specimens in the central 310-mm length.

Table 2 Results of tests

(a)conducted from 2002 to 2006 by the authors

specime name	subjected axial load [kN]	experimental result				
		maximum lateral stregnth [kN]	maximum value until losing axial load carrying capacity			
			lateral deflection [mm]	lateral deflection angle [rad]	axial deformation [mm]	axial strain
P-3	400	149	7.2	0.020	3.33	0.018
P-4	300	134	9.0	0.025	6.56	0.036
H-3	400	137	6.3	0.018	1.96	0.011
H-4	200	110	7.3	0.020	7.07	0.039
W-3	300	111	9.0	0.025	2.08	0.012
W-4	500	114	5.4	0.015	2.55	0.014
S-3	300	117	9.0	0.025	2.74	0.015
W52-1	500	155	6.3	0.018	3.79	0.021
W52-2	350	137	9.0	0.025	7.55	0.042
W90-1	350	120	4.5	0.013	1.17	0.007
W90-2	200	109	6.3	0.018	1.07	0.006
D13W-1	300	122	10.8	0.030	8.27	0.046
D13W-2	500	130	5.4	0.015	2.65	0.015
D13W-3	500	116	5.4	0.015	4.57	0.025
D13S-1	300	110	7.2	0.020	3.52	0.020
D13S-2	500	126	4.6	0.013	1.81	0.010
φ4W-1	300	111	10.8	0.030	4.87	0.027
φ4W-2	500	108	3.6	0.010	1.95	0.011
WH-1	300	120	7.2	0.020	0.84	0.005
WH-2	500	134	5.4	0.015	0.81	0.004
SH-1	300	127	7.2	0.020	1.16	0.006
SH-2	500	139	5.4	0.015	1.22	0.007
WL-1	150	84.5	14.4	0.040	9.44	0.052
WL-2	300	86.7	7.2	0.020	6.27	0.035
SL-1	150	82.7	9.0	0.025	4.39	0.024
SL-2	300	87.2	7.2	0.020	4.10	0.023

(b)conducted after 2006 by the authors

specime name	subjected axial load [kN]	experimental result				
		maximum lateral stregnth [kN]	maximum value until losing axial load carrying capacity			
			lateral deflection [mm]	lateral deflection angle [rad]	axial deformation [mm]	axial strain
H52LL-1	300	82.1	5.4	0.015	6.47	0.036
H52LL-2	150	76.4	10.8/	0.030	6.00	0.033
H90LL-1	300	70.3	5.1	0.014	1.02	0.006
H90LL-2	150	73.9	10.8	0.030	4.47	0.025
S52LL-1	150	79.5	10.8	0.030	3.87	0.022
I52LL-1	300	101	9.0	0.025	4.92	0.027
I52LL-2	450	73.8	3.6	0.010	7.42	0.041
V78LL-1	675	176	5.8	0.016	5.45	0.020
V135LL-	675	166	3.6	0.010	3.24	0.012
V135LL-	337.5	153	4.7	0.013	7.42	0.027
L52LL-1	300	71.5	5.9	0.016	6.11	0.034
L90LL-1	300	74.0	5.2	0.014	2.65	0.015
L90LL-2	150	62.2	6.6	0.018	4.55	0.025

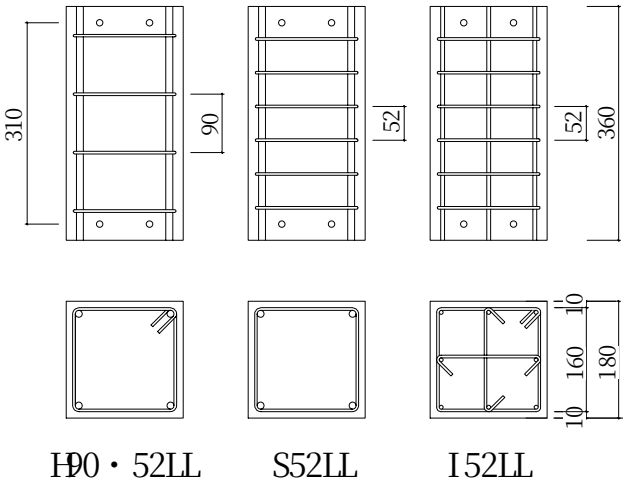

Fig. 3 Configuration and reinforcement of specimens (Table 1(b))

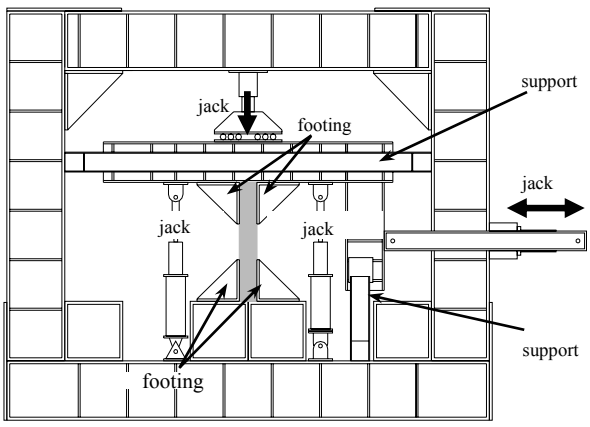

Fig. 4 Loading setup

Lateral loading tests were conducted using two vertical jacks to make the deformation at the top and the bottom of test specimens symmetrical. Specimens were subjected to lateral load reversals using one horizontal jack under a scheduled constant axial load shown in Table 2(b). The lateral load was reversed twice for each drift angle of 1/100, 1.5/100, 2/100, and 2.5/100 rad. The loading tests were conducted until the specimen lost its axial load carrying capacity.

Table 3 Properties of specimens and results of tests conducted by other researches

(a)specimens failing in shear

specime name	specimen properties		subjected axial load [kN]	maximum value until losing axial load	
	section [mm2]	height [mm]		lateral deflection [mm]	lateral deflection angle [rad]
B1	250×250	1000	2220	20.2	0.020
B2				39.9	0.040
B3				21.1	0.021
B4				41.1	0.041
B5				25.1	0.025
B6				26.5	0.027
B7				15.5	0.016
B8			3172	40.0	0.040
NO.1			1580	40.5	0.041
S3	300×300	900	3760	15.4	0.017
S4				33.6	0.037
S5				35.3	0.039
S7			3290	30.4	0.034
S9	250×250	1000	1620	39.5	0.040
IC-1	150×150	380	220	15.2	0.040
IC-2				15.2	0.040

(b)specimens failing in flexure

specime name	specimen properties		subjected axial load [kN]	maximum value until losing axial load	
	section [mm2]	height [mm]		lateral deflection [mm]	lateral deflection angle [rad]
NO.1	350×350	1750	3289	52.5	0.030
NO.2		875		17.5	0.020
NO.6	365×365	808	4230	32.6	0.040
NO.3	250×250	1000	2280	27.5	0.028
NO.4			2270	42.6	0.043
C-8	317×317	1500	2790	45.2	0.030
C-9				60.0	0.040
S6	300×300	900	3290	18.2	0.020
S8	250×250	1000	690	52.8	0.053
S10			2310	18.7	0.019
NO.8	200×200	600	666	9.4	0.016
L2	250×250	1000	1750	40.4	0.040
J4	220×220	1100	870	41.8	0.038
LC	250×250	1000	760	24.0	0.024
IC-3	150×150	380	440	15.2	0.040
IC-4				15.2	0.040

3.3 Tests conducted by other researchers

In order to study the feasibility of Eq. (1), the data of RC column specimen tests conducted by other researchers in which the specimens were loaded until they lost their axial load carrying capacities were

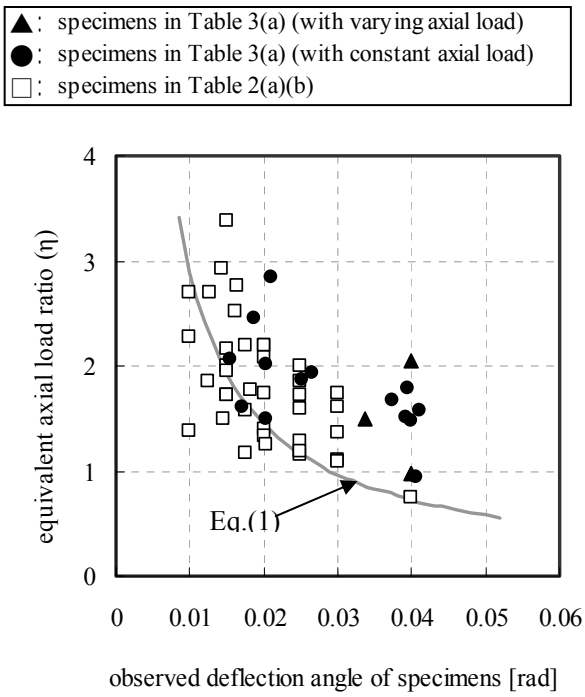

(a) comparison between equivalent axial load ratio and observed deflection angle when specimens lost their axial load carrying capacities

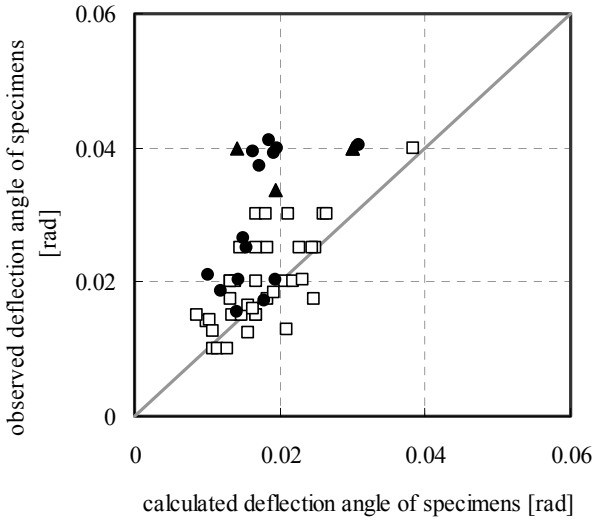

(b) comparison between test results and calculations by Eq.(1)

Fig. 5 Examination of accuracy of evaluating equation of lateral deflection angle when specimens lose their axial load carrying capacities of columns failing in shear

examined. Specimens were divided into two groups: shear failing columns and flexural yielding columns, which were determined by the calculated strength. Table 3(a) shows the section, the subjected axial load, and the test results of specimens failing in shear. Table 3(b) shows the section, the subjected axial load, and the test results of specimens failing in flexure. Details of these tests were reported by Kato et al. (2001) and Sasaki et al. (2002).

4. Feasibility of Equation (1)

Figure 5(a) shows the relationship between the observed deflection angle at the axial capacity point of specimens and the equivalent axial load ratio calculated using Eqs. (2) and (3). The solid line in the figure represents Eq. (1), which was empirically obtained using the experimental data shown in Table 2(a). Hollow square marks represent specimens in Tables 2(a) and (b), and solid marks represent specimens in Table 3. Specimens in Table 3 were divided into two groups: specimens with constant axial load and specimens with a varying axial load.

As described in Section 2, Eq. (1) shows good estimation for specimens listed in Table 2 with hollow square marks. In contrast, the solid line obtained by Eq. (1) is located around the lower limit of the data in Table 3 with solid marks. Although the figure shows a scattering, Eq. (1) is found to be effective for specimens in Table 3 including specimens with a varying axial load.

Figure 5(b) compares the observed deflection angle at the axial capacity point of specimens with the value evaluated by using Eq. (1) directly. The evaluation method using Eq.(1) is found to be effective as a conservative equation for evaluating the deflection angle at the axial capacity point of RC columns failing in shear including specimens with a varying axial load.

5. Application of Equation (1) to columns failing in flexure

The method for evaluating the deflection angle at the losing point of the axial load capacity for RC columns failing in flexure was proposed by Kato et al. (2001) and Sasaki et al. (2002). Figure 6(a) shows the relationship between the observed deflection angle at the losing point of the axial load capacity of the specimens failing in flexure shown in Table 3(b) and the calculated deflection angle proposed by Kato et al. (2001) and Sasaki et al. (2002). The accuracy is not bad. However, the method was based on flexural analysis using plane remained plane after bending, which was assumed to be different from the real behavior. Therefore, in this section, the applicability of the equation to RC columns failing in flexure is discussed.

It must be noted that there exist two types of axial load losing mechanisms for columns failing in flexure: i) shear failure after flexural yielding and ii) pure flexural failure. In this section, the applicability of the equation to RC columns failing in flexure is discussed on the basis of Eq. (1). In other words, only the first type of mechanism mentioned above is discussed.

Figure 7 shows the basic concept. Figure 7(a) shows lateral load–the lateral deflection angle relationship of a column failing in shear, in which the lateral deflection angle at the losing point of the axial

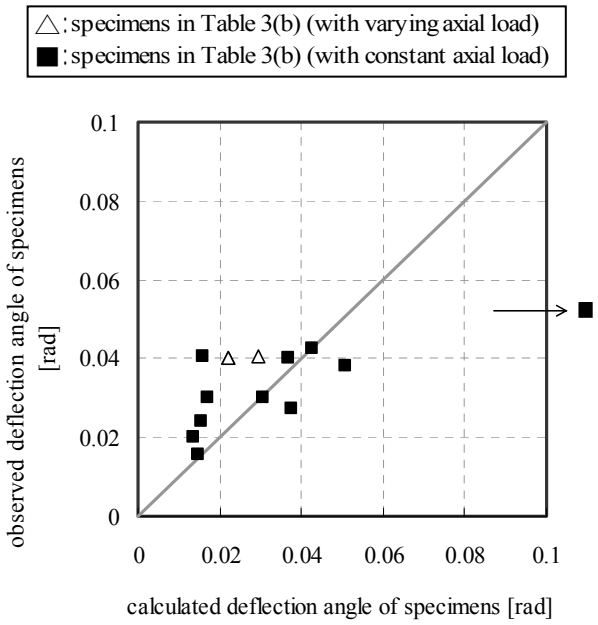

(a) method proposed by Kato et al. (2001) and Sasaki et al. (2002)

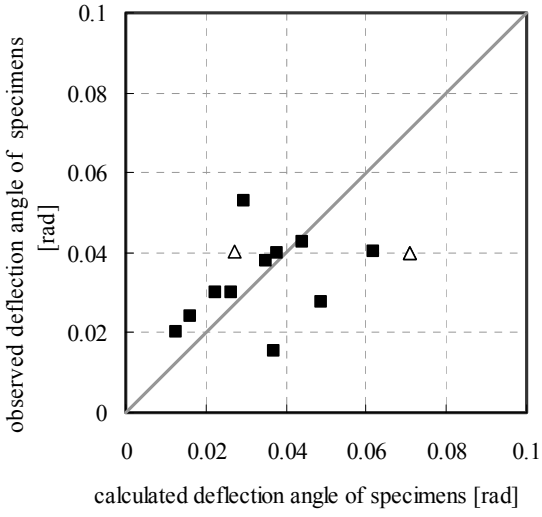

(b) method proposed in this paper

Fig. 6 Examination of accuracy of evaluation equation of lateral deflection angle when specimens lose their axial load carrying capacities of columns failing in flexure

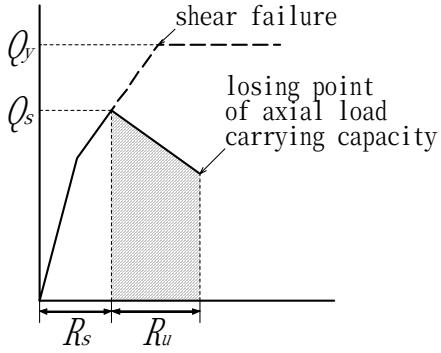

$R_{axis,s}=R_s+R_u$

(a)column failing in shear

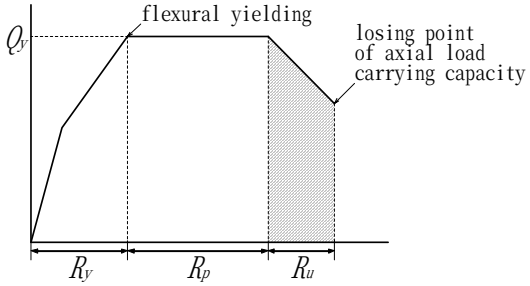

$R_{axis,f}=R_y+R_p+R_u$

(b)column failing in flexure

Fig. 7 Concept of evaluation equation of deflection angle when specimens lost their axial load carrying capacities of columns failing in shear and flexure

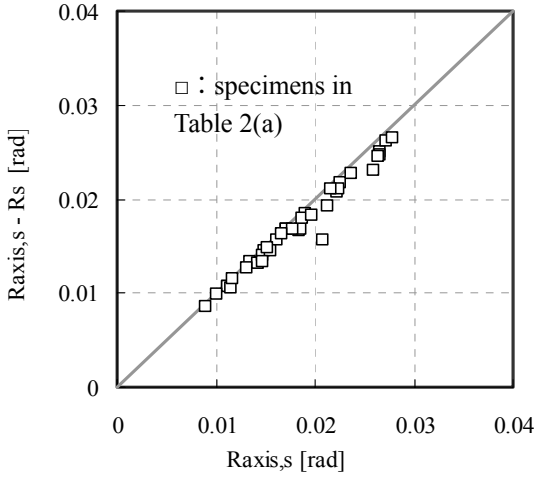

Fig. 8 Effects of deflection at shear failure on calculated deflection angle when specimens lost their axial load carrying capacities

load capacity of this column can be expressed by R_s + R_u, where R_s is the deflection angle at shear failure. In other words, the deflection angle $R_{axis,s}$ calculated by Eq. (1) is $R_s + R_u$ in this figure. In contrast, Figure 7(b) shows the relationship of a column failing in flexure, in which the lateral deflection angle at the losing point of the axial load capacity of this column is assumed to be expressed by $R_y + R_p + R_u$, where R_y is the flexural yielding deflection angle and R_p is the plastic deflection angle that depends on the deformation capacity of the column. Further, the most important assumption in this idea is that the deflection increment from after the column loses its deformation capacity to until the column loses the axial load capacity is equal to R_u of the shear failing columns shown in Figure 7(a).

However, there are two problems to be considered in this concept. The first problem is that the experimental data shown in Table 2(a) cannot be separated into R_s and R_u. In other words, only R_u cannot be evaluated. Therefore, it is necessary to examine the contribution of R_s to $R_s + R_u$ in these specimens. Figure 8 shows the relationship between $R_{axis,s} - R_s$ and $R_{axis,s}$, where R_s is obtained as the intersection of the calculated load-deflection behavior and the calculated shear strength (Fig. 7(a)). The figure shows that the contribution of R_s is negligible. This is because the flexural strength of these specimens was designed to be very high for experimental purposes.

The second problem is that in the case of the flexural failing column, the failure zone is usually concentrated on the end zone of the column, whereas the failure zone of the shear failing column usually occurs in the middle zone of the column (see inclined crack line in Figure 1). The difference in the position of the failure zone influences the effects of longitudinal reinforcing bars on the axial load ratio in general. Therefore, the contribution of longitudinal reinforcing bars to the axial load ratio is cancelled because these bars are subjected to compression and tension due to the presence of the moment of the end zone. Note that all longitudinal reinforcing bars affect the axial load ratio as shown in Eq. (4) because the effect of the moment is negligible in the case of shear failing columns.

Consequently, the equation for evaluating the lateral deflection angle at the axial capacity point for RC columns failing in flexure can be expressed as follows:

$$R_{axis,f} = R_y + R_p + R_{axis,s}' \quad (5)$$

where $R_{axis,s}'$ can be obtained as $R_{axis,s}$ using Eqs.(1)–(4). However, it must be noted that the contribution of longitudinal reinforcing bars to the axial load ratio is canceled in the case of flexural yielding columns ($A_s\sigma_y$ should be 0 in Eq. (4)).

R_y and R_p are the yielding deflection angle and the plastic deflection angle depending on the deformation capacity, which can be obtained using the existing evaluation methods. For example, R_y can be obtained using Eq. (6), in which the secant yielding stiffness degradation ratio α_y was proposed by Sugano (1970).

$$R_y = \frac{Q_f}{K_e \cdot \alpha_y} \tag{6}$$

$$\alpha_y = (0.043 + 1.64 \cdot n \cdot p_t + 0.043\frac{a}{D} + 0.33\eta_o)(\frac{d}{D})^2$$

where Q_f is the flexural strength, K_e is the elastic stiffness, n is the modular ratio, p_t is the tensile reinforcement ratio, a is the shear span, η_o is the axial stress divided by the concrete compressive strength, and d and D are the effective depth and the overall depth of the section.

In contrast, R_p can be evaluated by using the method proposed by AIJ (1999) for example. Eq. (7) represents the shear strength based on the truss and arch mechanism, in which R_p is quoted. In other words, Q_s represents the potential shear strength after flexural yielding. Consequently, R_p can be obtained as a suitable R_p to match the shear strength Q_s with the flexural strength Q_f in this method. Practically, the iteration is necessary until the same value of Q_s as that of Q_f is obtained by varying R_p.

$$Q_s = \min(V_{u1}, V_{u2}, V_{u3}) \tag{7}$$

$$V_{u1} = \mu \cdot p_{we} \cdot \sigma_{wy} \cdot b_e \cdot j_e + (\nu \cdot \sigma_B - \frac{5p_{we} \cdot \sigma_{wy}}{\lambda})\frac{b \cdot D}{2}\tan\theta$$

$$V_{u2} = \frac{\lambda \cdot \nu \cdot \sigma_B + p_{we} \cdot \sigma_{wy}}{3} b_e \cdot j_e$$

$$V_{u3} = \frac{\lambda \cdot \nu \cdot \sigma_B}{2} b_e \cdot j_e$$

$$\mu = 2 - 20R_p$$

$$\nu = (1 - 20R_p)(0.7 - \frac{\sigma_B}{200})$$

$$\lambda = (1 - \frac{s}{2j_e})(1 - \frac{b_e}{4j_e})$$

where b and D are the width and depth of the section, b_e and j_e are the effective width and the depth for the truss mechanism of the section, s is the spacing of the hoop, p_{we} is the effective hoop reinforcement ratio, σ_{wy} is the yielding strength of the hoop, σ_B is the concrete strength (unit: N/mm^2), θ is the angle of arch action, R_p is the plastic deflection angle determined by the plastic rotation of the hinge region. For more details, see Design Guidelines by AIJ (1999).

Figure 6(b) shows the relationship between the observed deflection angle at the losing point of the axial load capacity of specimens failing in flexure shown in Table 3(b) and the calculated deflection angle using Eqs. (5)–(7). The scatters of the figure are found to be better than those of Fig. 6(a), which shows the effectiveness of this method.

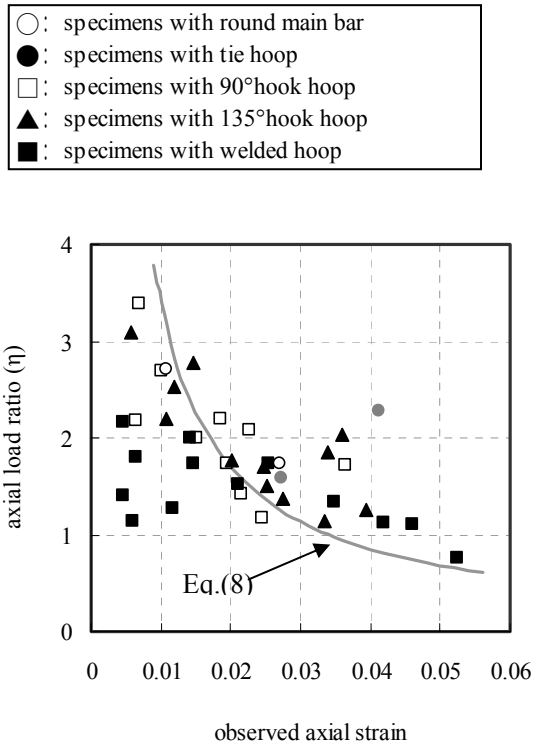

(a)comparison between equivalent axial load ratio and observed axial strain when specimens lose their axial load carrying capacities

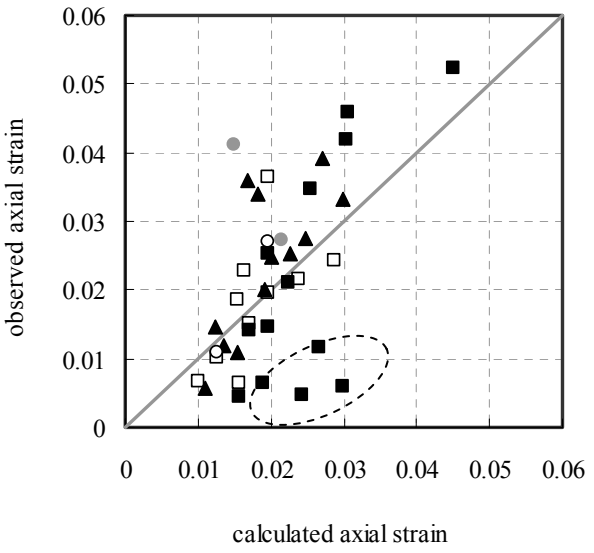

(b)comparison between test result and calculation

Fig. 9 Examination of accuracy of evaluation equation of axial strain when specimens lose their axial load carrying capacities of columns failing in shear

6. Trial to evaluate axial deformation at losing point of axial load carrying capacity

It is also important to evaluate the axial deformation at the axial capacity point because the role of

connecting beams and surrounding columns depends on the axial deformation at the axial capacity point of the failing column. In other words, in a practical building, the axial load is resisted by a combination of the columns and the connecting beams, which implies the importance of the compatibility of the axial displacement.

From this viewpoint, the trial to evaluate the axial deformation at the axial capacity point was carried out in this study although it is difficult to propose an accurate estimation for the axial deformation in general. In this study, the evaluation equation was examined by following the same approach as that used for evaluating the lateral deflection in Section 2 although it had a poor theoretical background for axial deformation.

Figure 9(a) shows the relationship between the observed axial strain at the axial capacity point of specimens shown in Table 2(a) and (b) and the equivalent axial load ratio calculated using Eqs. (2) and (3). As described previously, it must be noted that these specimens failed in shear, and the axial strain was obtained by dividing the axial deformation with the depth of the column section (D). The figure shows that the observed axial strain gradually increases with decreasing values of the axial load ratio. The solid line in the figure is an approximation expressed by Eq. (8).

$$\varepsilon_{axis,s} = \frac{0.034}{\eta} \qquad \left(\eta = \frac{{}_{e}N}{P_{fr,cal}}\right) \qquad (8)$$

Figure 9(b) compares the observed axial strain of specimens with the value calculated using Eq. (8) directly. This evaluation method (Eq. (8)) is found to be effective although the accuracy for columns with a welded hoop is bad. These specimens with a welded hoop include specimens with a large hoop spacing or high concrete strength (Table 1), which may lead to errors. Therefore, it is important to improve the accuracy of this equation for future works.

7. Conclusions and Scope for Future Work

1) The equation (Eq. (1)) for evaluating the lateral deflection angle at the losing point of the axial load capacity for columns failing in shear, proposed by Kato in 2006, was reexamined using specimens with a wider range of variables. The evaluation method was found to be effective as a conservative evaluation equation.
2) The equation for evaluating the lateral deflection angle at the axial capacity point for RC columns failing in flexure was proposed on the basis of the evaluation equation for columns failing in shear (Eq. (5)). The evaluation method was found to be effective.
3) The equation for evaluating the axial deformations at the axial capacity point for RC columns failing in shear was proposed (Eq. (8)). The evaluation method was found to be effective although the accuracy for columns with a welded hoop was bad. The specimens with a welded hoop include specimens with a large hoop spacing or high concrete strength, which may lead to errors. Therefore, it is important to improve the accuracy of this equation for future works.

References

1)Architectural Institute of Japan (1999). Design Guidelines for Earthquake Resistant Reinforced Concrete Buildings Based on Inelastic Displacement Concept. (in Japanese)

2)Kato, D. and Ohnishi, K. (2001) Axial load carrying capacity of R/C columns under lateral load reversals, The third U.S.-Japan Workshop on performance-Based Earthquake Engineering Methodology for Reinforced Concrete Building Structures, pp.231-239

3)Kato, D., LI Zhuzhen, Suga, K. and Nakamura, Y. (2004) Effects of Reinforcing Details on Axial Load Capacity of R/C columns, the 13-th World Conference on Earthquake Engineering, 2004, CD-ROM

4)Kato, D., LI Zhuzhen, Nakamura, Y. and Honda, Y. (2006) Tests on Axial Load Capacity of Shear Failing R/C Columns Considering Reinforcing Details (Relationship between Axial Loading Test and Lateral Loading Test), Journal of Structural and Construction Engineering, Architectural Institute of Japan, No.610, pp.153-159. (in Japanese)

5)Moehle, J. P. , Elwood, K. J. and Sezen, H. (1999) Shear failure and axial load collapse of existing reinforced concrete columns, The first U.S.-Japan Workshop on performance-Based Earthquake Engineering Methodology for Reinforced Concrete Building Structures, pp.233-247

6)Miyajima, Y., Tomita, Y.. LI Zhuzhen and Kato, D. (2007) Tests of axial load capacity of shear failing R/C columns to evaluate effects of reinforcing details, Proceedings of the Japan Concrete Institute, Vol.29, No.2, 2007, pp.79-84 (in Japanese)

7)Miyajima, Y., Abe, H. and Kato, D.(2008) Test of Axial Load Capacity of R/C Column Specimens with Various Size, Proceedings of the Japan Concrete Institute, Vol.30, No.2, 2008, pp.163-168 (in Japanese)

8)Nakamura T., Yoshimura M., Owa S. (2002) Axial load carrying capacity of reinforced concrete short columns with shear mode, Journal of structural and construction engineering, AIJ, No.561,pp193-100 (in Japanese)

9)Sasaki, J. and Kato, D. (2002) Evaluating Method of Crack Width, Crushing Area and Axial Load Carrying Capacity of R/C Columns, Proceedings of the Japan Concrete Institute, Vol.24, No.2, 2002, pp.253-258 (in Japanese)

10)Sugano, S. (1970) Experimental study on restoring force characteristics of reinforced concrete members, a thesis submitted to The University of Tokyo, The university of Tokyo, December 1970 (in Japanese)

11)Pujol, Santiago, Sozen, Mete and Ramirez, Julio (2000) Transverce reinforcement for columns of RC frames to resist earthquakes, Journal of Structural Engineering, April 2000, pp.461-466